University of Cincinnati

Date: 3/27/2013

I, Sumit Kumar Narendrakumar Jui , hereby submit this original work as part of the requirements for the degree of Master of Science in Mechanical Engineering.

It is entitled:

STUDY OF MICRO-ELECTROCHEMICAL DISCHARGE MACHINING (ECDM) USING LOW ELECTROLYTE CONCENTRATION

Student's name: **Sumit Kumar Narendrakumar Jui**

This work and its defense approved by:

Committee chair: Sundaram Murali Meenakshi, Ph.D.

Committee member: Anil Mital, Ph.D. P.E.

Committee member: David Thompson, Ph.D.

6934

Study of Micro-Electrochemical Discharge Machining (ECDM) using

Low Electrolyte Concentration

A thesis submitted to the

Graduate School

of the University of Cincinnati

in partial fulfillment of the

requirements for the degree of

MASTER OF SCIENCE

in the School of Dynamic Systems

of the College of Engineering & Applied Sciences

by

Sumit Kumar Jui

Bachelor of Engineering in Mechanical

Maharashtra Institute of Technology (Kothrud), University of Pune, India,

2008

March 2013

Committee Chair: Dr. Murali Sundaram

ABSTRACT

Demand for miniaturized products is ever increasing as they accomplish the task of providing the desired functionalities with high efficiency using minimalistic raw material. In order to execute functionalities like high strength and sustainability with minimal use of space, the raw materials used should possess good mechanical, chemical and physical properties. This requirement poses several challenges including high tool wear and lack of precision in the micromachining of such superlative engineering materials. Although, electrical discharge machining (EDM) and electrochemical machining (ECM) are well established nontraditional techniques to meet these challenges, they are restricted to electrically conductive materials. Several electrically non-conductive materials like ceramics and fiber-reinforced composites are increasingly being used in miniaturized pumps, reactors, accelerometers and many other biomedical devices. Micro Electrochemical Discharge Machining (micro-ECDM) has the capability to meet these challenges. However, machining high aspect ratio features on ceramics like glass still remains a formidable task due to overcut. Since electrolyte concentration plays an important role in overcut its effects on material removal needs to be studied in order to enhance the capability of this technology in machining complex and high aspect ratio features.

A micro-ECDM system has been designed and built in-house as a part of this research work. A mathematical model has been developed to understand the role of electrolyte concentration in material removal of the process. The model predicts overcut and quantifies the effect of electrolyte concentration in material removal. Experimental studies were conducted and the model was verified under varying machining parameters. The experimental values varied with the theoretical prediction in the range of 2-22%.

The mathematical model showed that reducing electrolyte concentration reduces overcut. In order to put this phenomenon to use several experiments were conducted to machine high aspect ratio holes on glass. Micro holes with an aspect ratio in the range of 9-12 have been fabricated which is more than 3-4

times that of reported in the literature. The effect of low electrolyte concentration on entrance and exit diameters of the micro-hole has been studied. Its effect on the overcut and taper of the micro-hole as well as tool wear has also been studied and reported. These studies proved that lowering the electrolyte concentration in micro-ECDM plays a major role in increasing the aspect ratio of the machined features.

ACKNOWLEDGEMENTS

Dr. Murali Sundaram is not just an academic advisor to me but he has always been a source of motivation during my research. He has shown me how important it is to question the obvious especially in the field of research. He has exposed me to an environment of top quality research and fulfilled my desire to do experimental work in the manufacturing domain. Words cannot justify my sense of gratitude towards him. I would like to thank him for his support and belief in me.

I like to sincerely thank Dr. David Thompson and Dr. Anil Mital for graciously accepting my request to serve on my thesis defense committee.

I thank Abishek Balsamy Kamaraj for the numerous discussions and the constructive criticism of my work which has helped me. I thank him for all his inputs and wish him all the best for his PhD endeavors.

I would like to thank Sagil James and Ryan Buffington for helping me out with the micro-ECDM setup. I will always be grateful to the Micro and Nano Manufacturing Laboratory along with its inhabitants Anuj Dabholkar, Himanshu Ingale, Varun Sharan Kumar, Guangfeng Hou and Shiv Shailendar for their inputs and not so funny banter. I thank my roommate's Gaurav Mukherjee and Rigwed Tatu to bear with me for two years which is not an easy task. I thank the University of Cincinnati Cricket Club and its members to make my stay so memorable.

I am grateful to the University of Cincinnati for providing me with a generous scholarship reducing my financial burden.

Finally, I am grateful to the most important people in my life, a selfless mother, an ever supportive father and a constantly critical sister who motivated me to pursue graduate studies. I dedicate this thesis to Mrs. Etu Jui, Mr. Narendra Kumar Jui and Susmita Kurup.

TABLE OF CONTENTS

LIST OF FIGURES

LIST OF TABLES

LIST OF NOTATIONS / NOMENCLATURE

I_m	mean machining current in milliamperes
Q	heat supplied to the system
Q_j	joule heat in watts
K	thermal conductivity in (W/mK)
ρ	density in (kg/m^3)
c	specific heat capacity in (J/molK)
P	heat supplied in watts
V	machining voltage in (V)
V_d	water decomposition potential in (V)
R	inter-electrode resistance in ohms
q	energy used for material removal in watts
t	total machining time in (s)
r	radial distance in microns
I_p	peak current in milliamperes
C_f	time correction factor

CHAPTER 1

1. Introduction

Most modern products are required to be conveyable, strong and support various functionalities. Miniaturized products score heavily on all of these accounts. These products have numerous applications in medical devices, electronics, biopharmaceuticals and various other micro parts of engineering devices [1]. Advanced engineering materials have the capability to provide high strength along with occupying less space. Micromanufacturing of such difficult to machine materials is a big task due to such high strength as it leads to severe tool damage. In order to suffice the ever growing demand of such miniaturized products, micromachining technologies need to be brought at par.

Electrical discharge machining (EDM) is a well-established micromachining technology. Although a lot of research has been done in this field, one of the biggest stumbling block is its difficulty to machine electrically nonconductive materials [2]. Electrochemical machining (ECM) is another technology which provides excellent surface finish and machining tolerances but suffers from the same drawback as of EDM [3]. Chemical processes like etching are often slow and quite expensive [4]. Laser and ultrasonic machining have limited machining depth and ultrasonic machining also causes high tool wear [5, 6]. Electrochemical discharge machining (ECDM) is a process that has the ability to micromachine electrically nonconductive materials with good speed and accuracy [7].

ECDM is a non-contact machining process with the capability to machine electrically nonconductive, high strength, high stiffness and chemically resistive materials. It is also known as spark assisted chemical engraving (SPACE), electrochemical arc machining (ECAM) and electrochemical spark machining (ECSM). It can produce complex 3 dimensional geometries on hard to machine materials like glass with good precision [8]. As ECDM is a thermal process, machining of the work material leads to some heat affected zones and surface cracks. However, these disadvantages can be diminished by using a pulsed power source with suitable frequency and duty ratio [9]. Tool wear is relatively low as compared to most other nontraditional manufacturing process [10]. It is possible to achieve high machining reproducibility with proper investigation into electrolyte concentrations, machining voltage, pulse on/off-time and feed rate [11].

1.1. Motivation

The focus of this research was to understand the effect of electrolyte concentration on the material removal. Cook et al. were the first research group to study the influence of electrolyte concentration on the material removal rate [12]. They reported that material removal rate increases with electrolyte concentration.

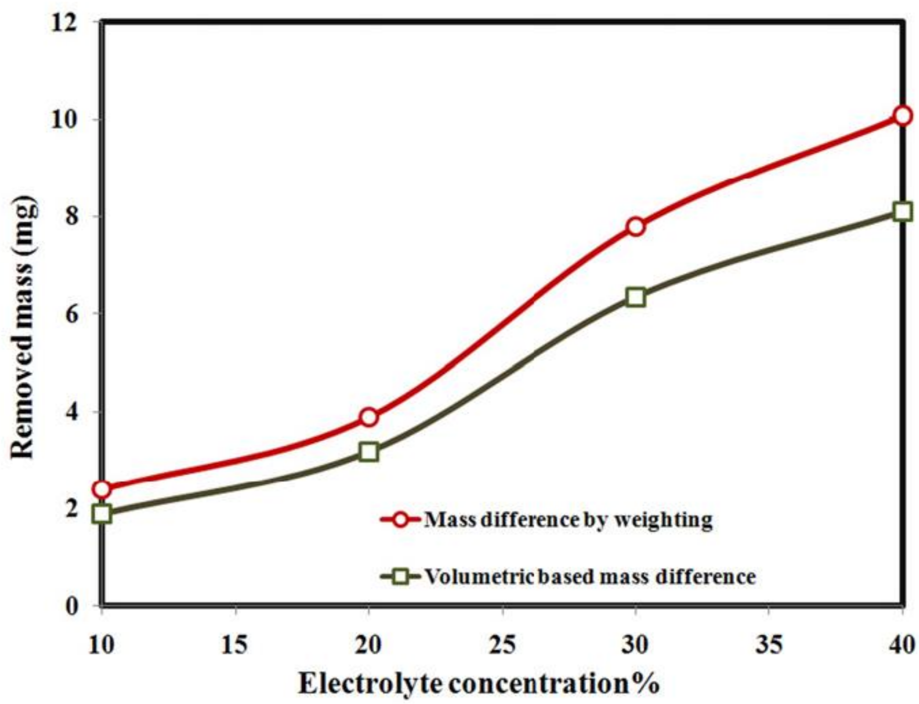

Figure 1: Effect of electrolyte concentration on material removal rate [13].

In order to study the effect of low electrolyte concentration on the material removal in micro-ECDM a mathematical model has been developed. The model predicts the overcut according to electrolyte concentration. It has been experimentally verified.

The effect of low electrolyte concentration on machining microholes in glass has been studied and reported. Its effect on the entrance and exit diameters, overcut and taper of the hole has been studied. Its effect on tool wear has been reported. The surface roughness of the machined samples has been studied.

1.2. Objectives

The objectives of this research are to

1. Model the effect of low electrolyte concentration on overcut in micro-ECDM
2. Study the effect of low electrolyte concentration on machining microholes in ECDM

1.3. Outline

The thesis is organized as follows: Chapter 1 gives an introduction to the topic and the process. It is followed by a comprehensive literature review of the work that has been done in Chapter 2. Chapter 3 describes the design and make of the micro-ECDM setup built in-house. A mathematical model is described in Chapter 4 which quantifies the effect of electrolyte concentration on the material removal. Using the understanding from the mathematical model Chapter 5 describes the fabrication of high aspect ratio microholes on glass. The conclusions drawn from this work are explained in chapter 6.

CHAPTER 2

2. Literature Review

2.1. Introduction

ECDM is a nontraditional machining process capable of machining a wide range of materials, especially nonconductive ceramics. The process involves a DC voltage being applied between the electrodes immersed in an electrolytic solution as shown schematically in Figure 2. The process can be explained with the help of the current and voltage characteristics. Figure 3 shows the variation of current

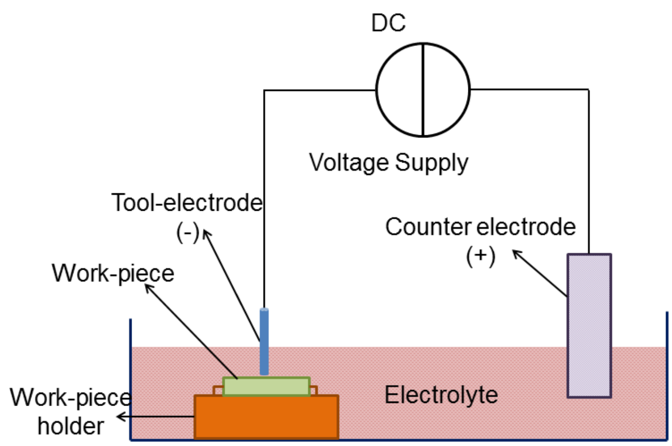

Figure 2: Schematic of an ECDM setup.

with voltage. As the voltage between the two terminals is increased hydrogen bubbles are generated at the cathode (From point A-C in Figure 3). Beyond this region, the current drops (point C in Figure 3) at a particular point, known as critical point, and discharges appear at the tool surface inside the electrolyte. The current and voltage at this critical point are known as critical voltage and critical current. At the critical voltage the bubbles begin to coalesce in a manner so as to separate the tool from the electrolyte which causes the discharges. Around 1A/mm^2 of current density is required to generate the gas film around the tool [14].

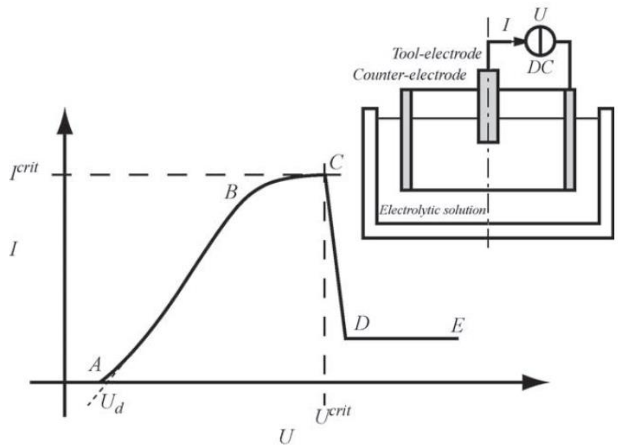

Figure 3: Typical voltage and mean current characteristics during ECDM [7].

2.2. Process Capabilities

Fabrication of holes was one of the early applications of electrochemical discharge machining [15]. The process is capable of drilling holes as small as 12 µm [16]. Many research groups have machined holes in the range of 100 µm to 1000 µm. A comprehensive report of the machined features is represented in table 1.

Table 1 : Overview of published reports in ECDM machining (After [7])

	Micro-hole drilling	3D structuring	TW-ECDM
Glass	100-500 µm, 1-2 mm	100 µm × 1 mm	1-10 mm
Quartz	1-3 mm		1-10 mm
Ceramics	100-500 µm, 1 mm		1-10 mm
Composites	1 mm		[13, 17]
Granit	25 mm [18]		

The shape of the hole depends on the geometry of the tool. Wire electro discharge grinding (WEDG) has been used to produce tools of various sizes and shape that fabricate holes with cylindrical, triangular and square shapes [19]. The lack of availability of electrolyte in the machining zone in case of deep holes is a major stumbling block. This leads to decrease in material removal rate with increase in hole depth and results in increase of the local temperature. Increase in temperature may cause surface damage by the formation of thermal cracks. Vibration of the tool electrode in the vertical direction resolves this issue to a certain extent [20, 21]. Rotating the tool electrode increases the machining depth, prevents circularity errors and improves material removal rate [21-23]. Exocentric tools have been used to increase the machining depth of the process [22]. Abrasive cutting tools have been used to have better the efficiency of the process. This has been possible as a constant gap is maintained between the tool and the work material due to the abrasives embedded in the tool [24]. The process is capable of producing many complex 3D structures which will be discussed towards the latter half of this chapter.

2.3. Electrolytes

The temperature and concentration of the electrolyte plays a vital role in the material removal. Material removal increases with the electrolyte temperature as well as concentration to a certain extent [18]. The electrolytes that have been widely used so far for the process are NaOH, KOH, NaCl, $NaNO_3$, NaF, HCl and H_2SO_4. NaOH and KOH are most common due to their superior surface finish and material removal rate. Surface finish can be further improved by the use of certain molten salt electrolytes [18]. The type and concentration of electrolyte has an effect on surface roughness of the machined sample [23]. Heating the electrolyte to 60-80°C improves performance along with adding abrasive particles [14]. The standard electrolyte concentrations reported in the literature are 2.5M, 5M and 7M. In this study, we used NaOH as the electrolyte due to its superior surface finish qualities on glass.

2.4. Tool

The shape of the tool has a strong influence on the geometry of the machined hole [19]. Flat side wall shaped tool has been reported to perform better as compared to cylindrical tools. Figure 4 shows the geometrical shapes of a cylindrical and a flat side sidewall tool.

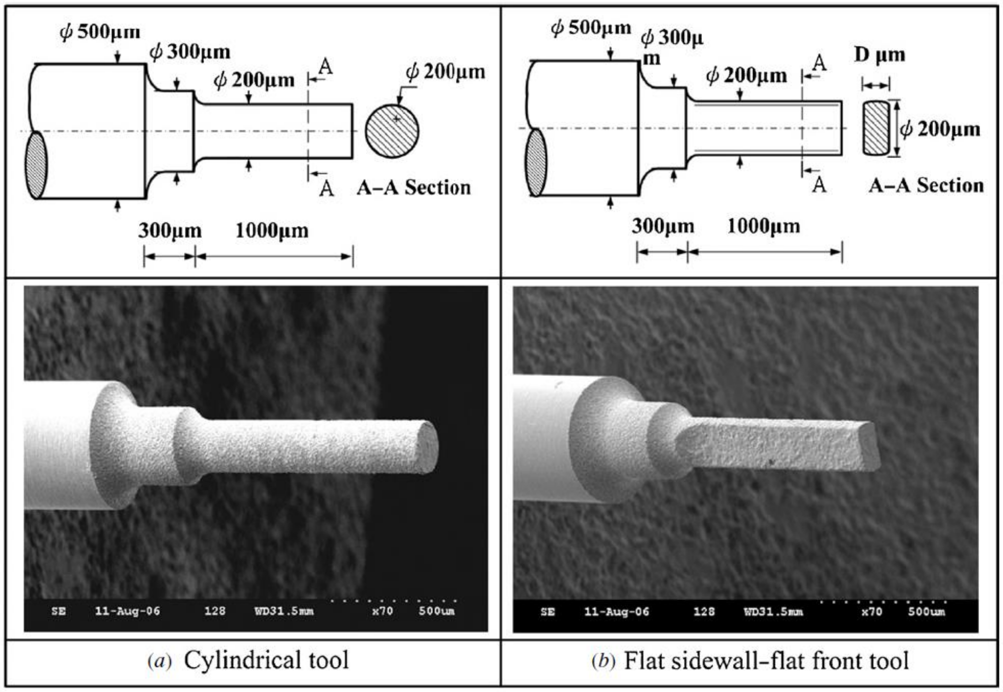

Figure 4: Geometrical shapes of various tools [8].

The flat sidewall tool helps in machining holes with reduced entrance diameters as compared to cylindrical tools thus improving the machining accuracy [25]. Figures 5 and 6 show the microholes machined by both tools.

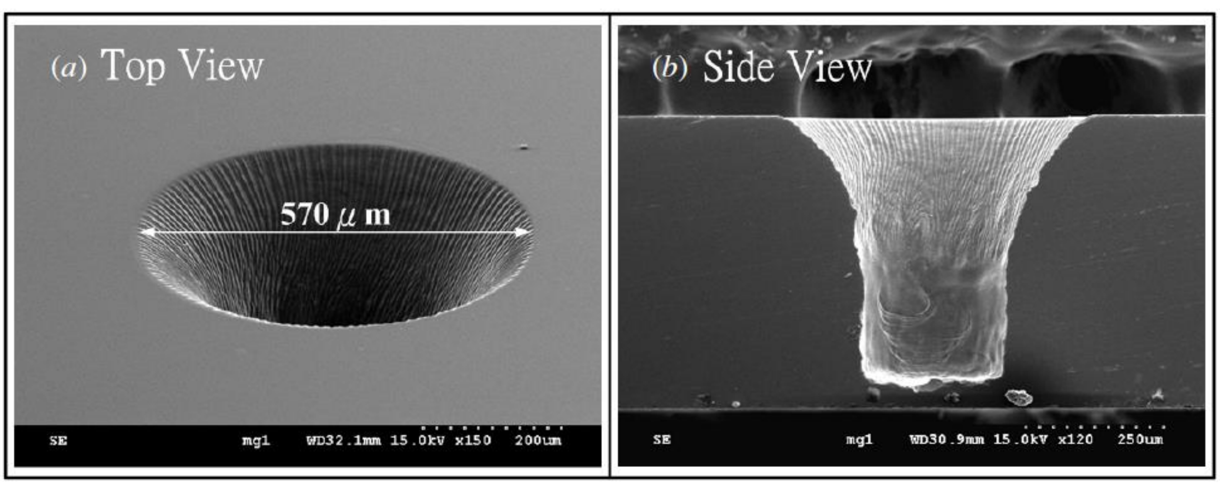

Figure 5: Microhole machined by cylindrical tool at 40V and 500 rpm [25].

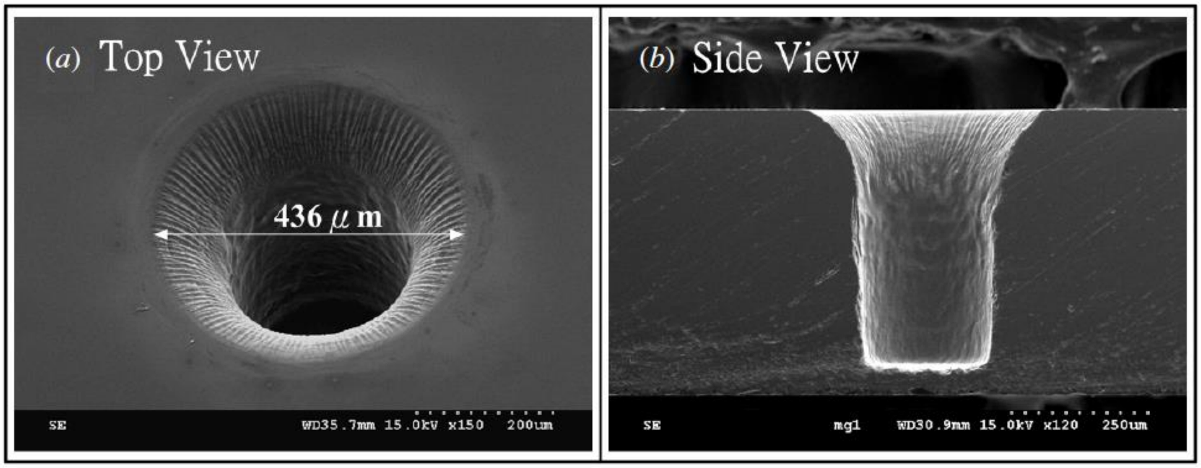

Figure 6: Microhole machined by flat sidewall tool at 40V and 500 rpm [25].

Spherical tool electrodes also perform better than cylindrical tools. They provide higher machining depth with comparatively small entrance diameters [26].

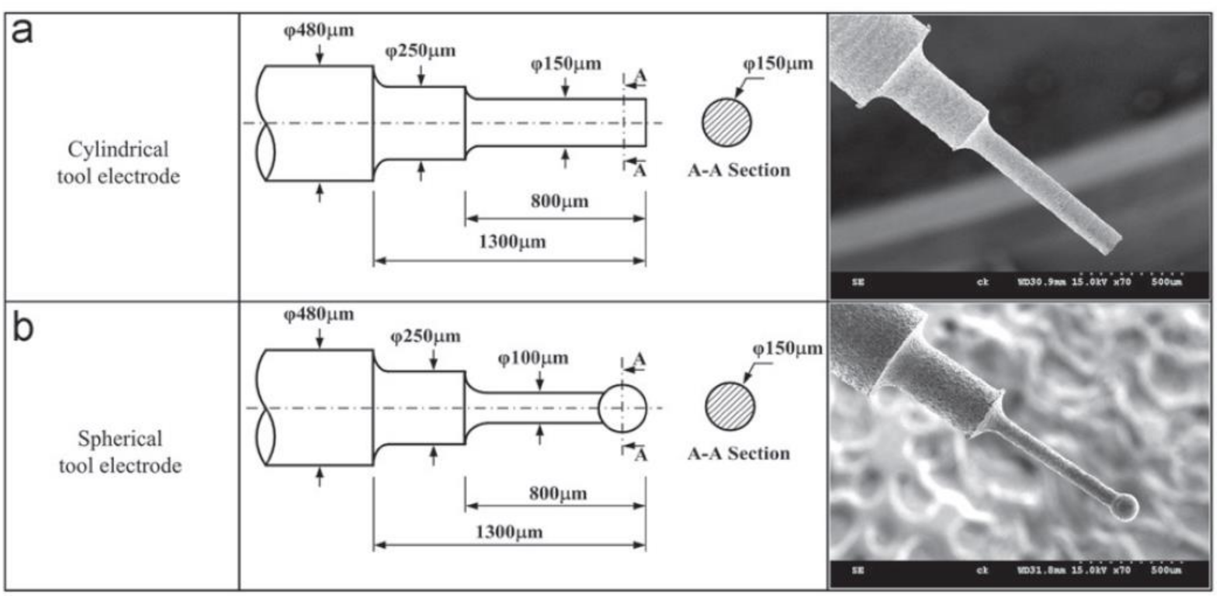

Figure 7: (a) Cylindrical tool electrode (b) Spherical tool electrode [26].

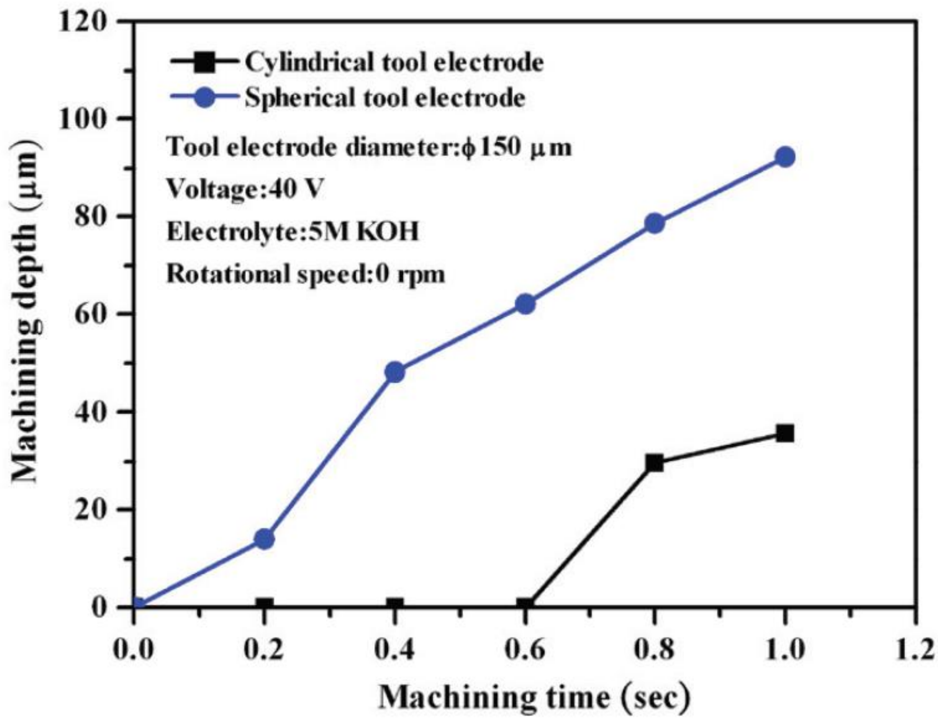

Figure 8: Initial machining status of different tool electrodes [26].

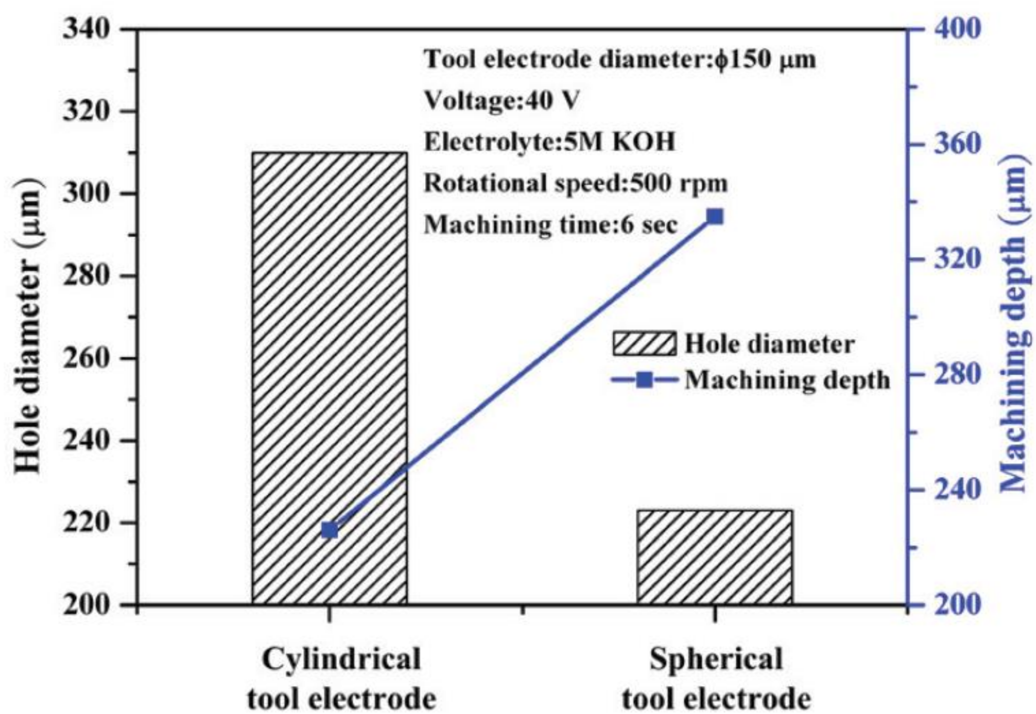

Figure 9: Effect on hole diameter and machining depth [26].

Tools with higher thermal conductivity consume more heat resulting in reduction in the energy available for the machining process. The material removal increases in the discharge regime while it decreases in the hydrodynamic regime when tools with high thermal conductivity are used [27]. Thermal expansion and tool wear for tungsten, steel and stainless steel has been studied and reported. Stainless steel has the highest thermal expansion while tungsten has the highest tool wear [10]. Discharges from side of the tool are one of the major reasons in increase of overcut. Side-insulated tools have been used and the reports show that it can reduce overcut to a great extent [28].

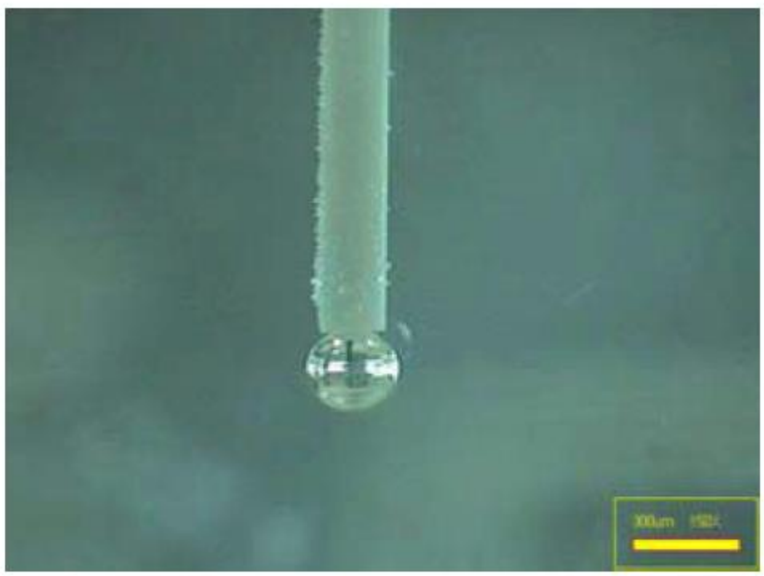

Figure 10: Image of the side insulated electrode [29].

2.5. Process modeling and simulation

The first theoretical model for the process was developed by Basak et al [30, 31]. The model predicts the onset of the discharges by predicting the critical voltage. The model compares the ECDM process to the switching off phenomenon in electrical circuits. However there are few deficiencies in the model namely [7] :

- Critical resistance is assumed rather than predicted by the model
- Electrode geometry plays a role on critical voltage which is not explained by the model
- The model fails to explain the bubble formation phenomenon

A similar study on the onset of the discharge mechanism was carried out by Liu et al. [32]. The process is compared to EDM using a metal matrix composite as the machining sample. A thermal model to predict the machining depth has been developed [33]. The model provides unsatisfactory results when the machining voltages are less than 25V. The model by Wüthrich et al. explains the bubble formation phenomenon and its effect on the critical parameters [34, 35]. The model also explains the dependence on tool diameter. Gas film thickness has been studied and controlled by some research groups [36, 37]. The effect of wettability of electrodes on the process is explained with the help of a model [38]. Finite element models have been developed to predict the material removal rate with respect the temperature distribution in the work material [39, 40]. The gas film formation for a side insulated electrode has been modeled [29].

2.6. Outcome

ECDM is a potential method to micromachine difficult to machine nonconductive ceramics. Several studies have been conducted however the actual effect of electrolyte concentration on the material removal has not been quantified. The use of electrolyte concentrations of up and above 2.5M has been reported. The literature does not explain the effect of electrolyte concentration on the overcut. It does not study the use of low electrolyte concentration (~1M) to machine using ECDM. The material removal rate increases to a certain point with the increase in electrolyte concentration. So reducing the electrolyte concentration might help in fabricating high aspect ratio features reducing overcut.

A detailed study on the effect of low electrolyte concentration on machining of glass has been reported in this research work. An analytical model was developed to quantify the effect of electrolyte concentration on overcut. In order to reduce tool wear for developing the process model, the tools were insulated with enamel.

High aspect ratio machining of glass has been performed in this research work. The effect of electrolyte concentration on taper has been studied. The surface finish of the samples and along with tool wear has been reported.

CHAPTER 3

3. Design of the micro-ECDM setup and preliminary machining studies

3.1. Introduction

A micro-ECDM system has been built in-house as a part of this work. In order to be able to machine in the micron scale certain design requirements and capability of the system components were considered. A schematic layout of the system is shown in the figure 11.

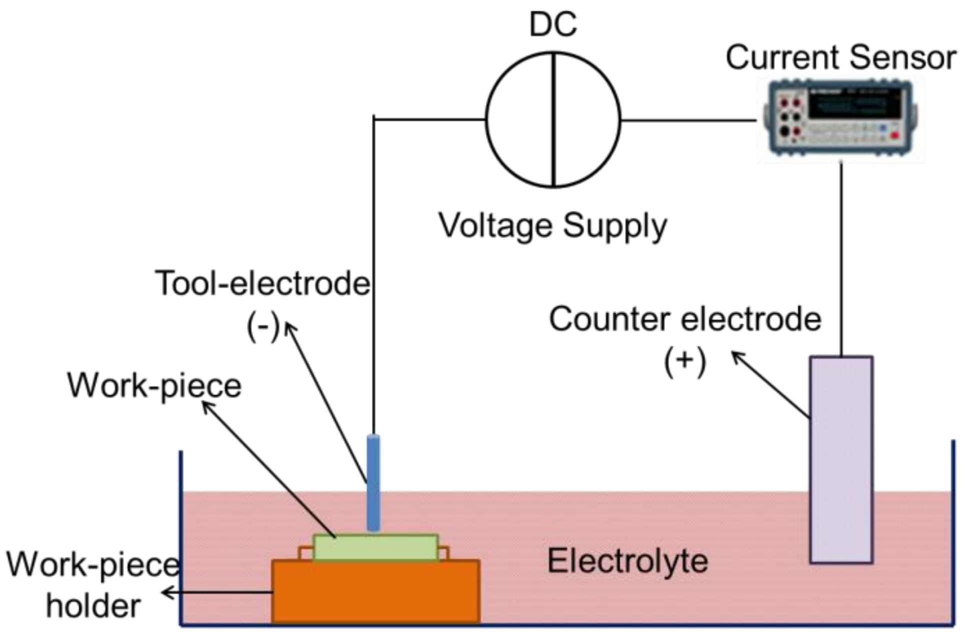

Figure 11: ECDM schematic.

The assembly consists of:

- DC power supply
- XYZ-LSMA System
- ST3 controller
- Anode
- Cathode (Tool-electrode)
- Tool Holder

- Electrolyte
- Work piece holding mechanism
- Electrolyte container
- Current Sensor

The following section details the design and capability of the system components.

3.2. System Components

DC power supply

A DC power supply is required to build an ECDM setup. For advanced capability a pulsed DC power supply is more suitable. The current density required for the discharges is around 1A/mm^2. The power supply is needed to supply voltages and current that is suitable to build the gas film around the tool electrode.

Features:

- Capable of supplying 113V and 1.3A
- Capable of being used in series for higher power requirements
- Digital control via USB/GPIB/RS-232C/RS-485
- Lock function
- Constant voltage/current mode

XYZ-LSMA System

The XYZ precision motion system is capable of travelling 13 mm in each of the three directions. A Stepnet ST3 stepper motor has been used to drive the system simultaneously in all the directions. The system has a resolution of 0.15 µm. The load carrying capacity of the system in the vertical direction is 3kg while in the horizontal direction it is 10kg. For its high stability and monolithic design the device is suitable in micromanufacturing systems.

Features:

- Direct motion prevents sliding pulleys, damage to lead screw and stretching belts
- Zero maintenance
- High repeatability (0.0001″) and accuracy (0.0005″)
- High flexibility

ST3 controller

The controller provides complete over motion in the XYZ directions simultaneously. Motion signals are sent to the controller by a computer (LabVIEW interface) through a RS232 port. ASCII codes were used to send motion signals to the controller. The controller can also provide acceleration to the drives.

Anode

The anode should be large to minimize anodic dissolution. It should be resistant to the electrolyte. The geometry of anode should avoid variance in the inter-electrode resistance [14]. The anode geometry should also minimize the inter-electrode resistance so that more energy is available for the machining process. A rectangular tool steel block is used as anode.

Cathode (Tool-electrode)

Tool should be stiff to avoid bending forces [14]. Material should be resistant to the electrolyte. Materials with higher thermal conductivity should be avoided so as to avoid the energy lost in heating the tool. Tungsten rods of 300 µm are used as cathode.

Dremel

A dremel capable of rotating at 10,000 rpm is used for holding the tool. Tool rotation improves circularity of the machined holes and increases machining depth.

Electrolyte

The conductivity of electrolyte is responsible for forming the gas film. The electrolyte etches the work material at high temperatures. Due to this property it is best suited to choose the electrolyte according to the work material being machined. As sodium hydroxide (NaOH) is reported to be having good results for machining glass, it was chosen as the electrolyte.

Electrolyte container

The container material should be chemically inert to avoid any reactions with the electrolyte. It should preferably be of a transparent material so that the machining activity could be observed. It should encircle the electrodes in such a way that no electrolyte should be spilt outside during machining activity. It should be designed in such a way that the electrolyte should be exposed only to the electrodes avoiding other parts of the system. It should be strong enough to hold a fixture for clamping purposes. In the present study, a container made up of glass has been used.

Multimeter

Machining current in the ECDM setup is of the order of milliamps. The breakdown of the gas film and its reformation occurs within milliseconds. This information can be captured with the help of a sensitive current reading device. A Tektronix multimeter was used to measure the current in the system.

Features:

- Accuracy of 0.015%
- Voltage range of 200 mV - 1000 V with 1 μV resolution
- Current range of 200 μA – 10 A with 1 nA resolution

- Resistance of 200 ohms – 100 megaohms with 1 milliohm resolution

3.3. Preliminary micromachining studies using ECDM

The machining parameters used for the preliminary studies are

Table 2: Machining parameters for preliminary study

Parameters	Value
Voltage	50 V
Electrolyte	2.5M, 5M, 7.5M NaOH
Tungsten tool Ø	300 µm
Immersion depth	300 µm

Barium Titanate

Barium titanate ($BaTiO_3$) is a dielectric material primarily used in capacitors. It has been used in transducers and several microphones. A through hole was machined with ease on a 1mm thick plate.

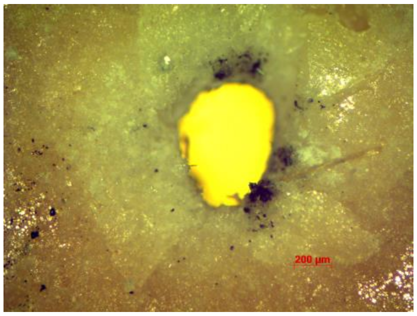

Figure 12: Through hole in Barium Titanate of 1mm thickness.

Borosilicate Glass

Borosilicate glass is an electrically nonconductive ceramic material. It has numerous applications in engineering, biomedical, medicine and many other fields. A through hole was made in a glass slip of 150 µm thickness.

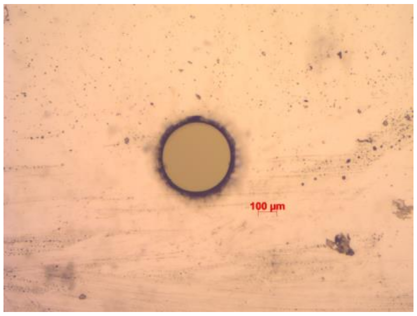

Figure 13: Through hole in Borosilicate glass of 1 µm thickness.

The preliminary machining studies showed that overcut increased with the electrolyte concentration. The machined hole diameter increased from 200µm to 250µm with increase in concentration from 5M to 7.5M NaOH. In order to understand this phenomenon a mathematical model was developed. The following chapter describes the model and its experimental verification.

CHAPTER 4

4. Mathematical Modeling of micro-ECDM

4.1. Introduction

In this chapter a mathematical model that predicts overcut is presented. The model enables us to quantify the effect of concentration on overcut in ECDM. It also aids in analyzing how the different machining parameters such as machining time, machining voltage and material properties affect the material removal. From the previous chapter we understand that concentration of the electrolyte has an effect on the overcut. Only limited studies have been performed on the effect of concentration in the ECDM process as noticed in the literature review. Hence modeling the material removal is important in order to understand and improve the process capability.

Although there are several models explaining the onset of sparks and the material removal mechanisms as mentioned in the literature review chapter, none of them quantify the effect of electrolyte concentration on overcut. Understanding this effect would help in controlling overcut thus increasing machining accuracy. The aspect ratio of machined features could be increased with this knowledge thus enhancing the capability of the process.

The assumptions and theory behind the model have been explained in the following section. Predictions made by the model were experimentally verified as discussed in section 4.4.

4.2. Process Modeling

It is hypothesized that ECDM of glass is a combination of thermal and chemical phenomenon [41]. Glass reacts with sodium hydroxide to form sodium silicate at elevated temperatures as given in equation below [42],

$$2NaOH + SiO_2 \rightarrow Na_2SiO_3 + H_2O \tag{1}$$

During ECDM, the thermal energy provided by the sparks is responsible for the temperature rise of the work material. This temperature rise accelerates the given reaction [43]. The process mechanism is shown in figure 14.

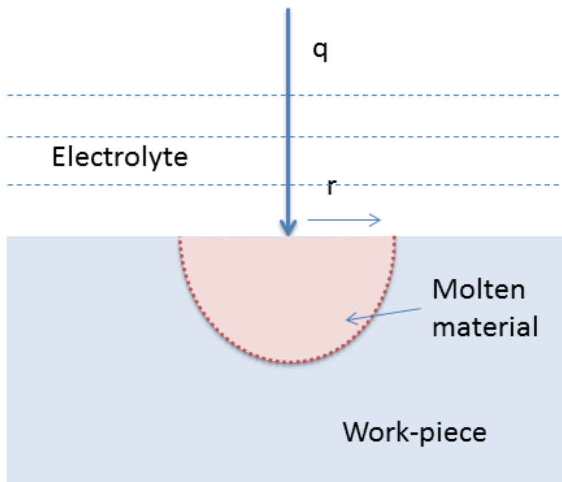

Figure 14: Point Heat Source.

The point heat source emits a heat power (Q) that is used in the machining process.

Some simplification assumptions were considered while arriving at the micro-ECDM model:

- The heat supplied by the electrochemical discharges to the work material is approximated as a point heat source.
- Electrolyte is always available in the machining zone.
- Work material is considered to have constant physical and thermal properties over variation of temperature.
- The work piece is assumed to be infinitely large.
- Heat is dissipated only by conduction i.e. convection and radiation losses are negligible.
- Heat dissipation during the spark off time is negligible.
- Convection and radiation losses are negligible.

The heat power (Q) supplied to the system is given by,

$$Q = V \times I_m \tag{2}$$

Where,

V → machining voltage,

I_m → mean machining current

The energy lost due to joule heating (Q_j) is given by,

$$Q_j = I_m^2 \times R \tag{3}$$

Where,

R → inter-electrode resistance of the electrolyte

The energy used for the material removal (q) is given by,

$$q = Q - Q_j \tag{4}$$

In the region outside the heat source the temperature distribution follows,

$$\frac{\rho c}{K}\frac{\partial T}{\partial t} = \nabla^2 T \tag{5}$$

Where,

ρ → density of material,

c → heat capacity,

K → thermal conductivity

The properties of glass were taken as K = 1.14 W/mK, ρ = 2230 kg/m^3 and c = 750 J/kg.K [44]

The solution to the above equation with a continuous point source is given by [45],

$$T(r,t) - T_0 = \frac{q}{4\pi Kr} erfc\left(r \times \sqrt{\frac{\rho c}{4Kt}}\right) \tag{6}$$

Where,

$t \rightarrow$ total machining time,

$r \rightarrow$ overcut as shown in schematic (figure 14)

The process consists of intermittent sparks and so a time correction factor is introduced. It is the ratio of mean machining current (20 milliamps) to peak current (1A).

$$C_f = \frac{I_m}{I_p} \tag{7}$$

where,

$I_p \rightarrow$ peak current

So, corrected machining time t is given by,

$$t = C_f \times t \tag{8}$$

This correction is based on the earlier assumption that the temperature of the workpiece does not reduce during the gap between two sparks as this time is very small. To confirm the applicability of this assumption 2D finite element simulation of the process was performed using ANSYS software. A 1 cm X 1 cm block of borosilicate glass was modeled and subjected to an intermittent heat load simulating a spark. A total of 50 sparks lasting 1µs with a gap between sparks of 400 µs were simulated. The temperature at a point 200 µm from the point source of heat was monitored during the simulation as shown in the Figure 15. From this it is clear that the gap between sparks is small enough to not cause any reduction in the temperature during the gap between sparks.

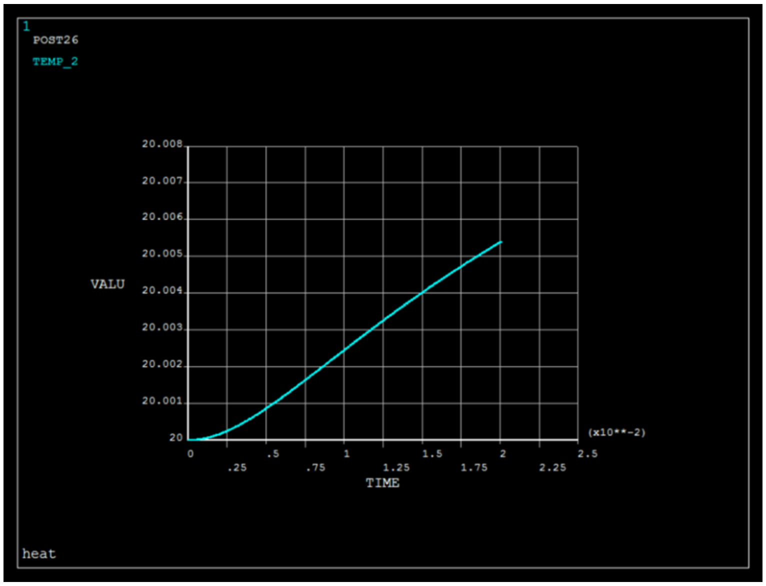

Figure 15: FEM simulated temperature rise of workpiece 200 µm from point heat source.

By substituting (2), (3), (4) and (8) in (6), we have,

$$T(r,t) - T_0 = \frac{(V \times I_m - I_m^2 \times \mathrm{R})}{4\pi Kr} erfc\left(r \times \sqrt{\frac{\rho c}{4KC_f\, t}}\right) \tag{9}$$

Some of the parameters in this model such as, electrolyte resistance and machining current are electrolyte concentration dependent and need to be obtained from experiments. This is explained in the next section along with the experimental validation of the model.

4.3. Experimental setup for verification of model

Experiments were carried out under varying electrolyte concentrations to measure the values of resistance and machining current of the process. The current at each voltage step of 1V was measured. The tool was not rotated during the experiments. The measurement was carried out till 60V to average the machining current after the onset of sparks. Three measurements were taken for each concentration in order to minimize the experimental errors.

Resistance was calculated as the ratio of average voltage and current in the ohmic region from figure 16.

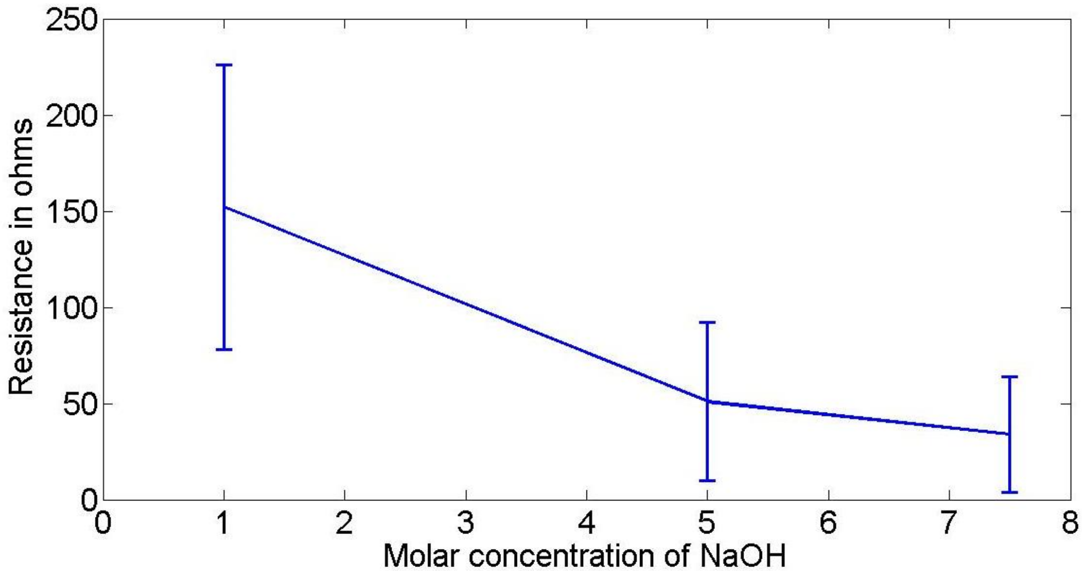

Figure 16: Resistance vs Electrolyte Concentration.

Machining current was taken as the average of the values measured after the onset of sparks.

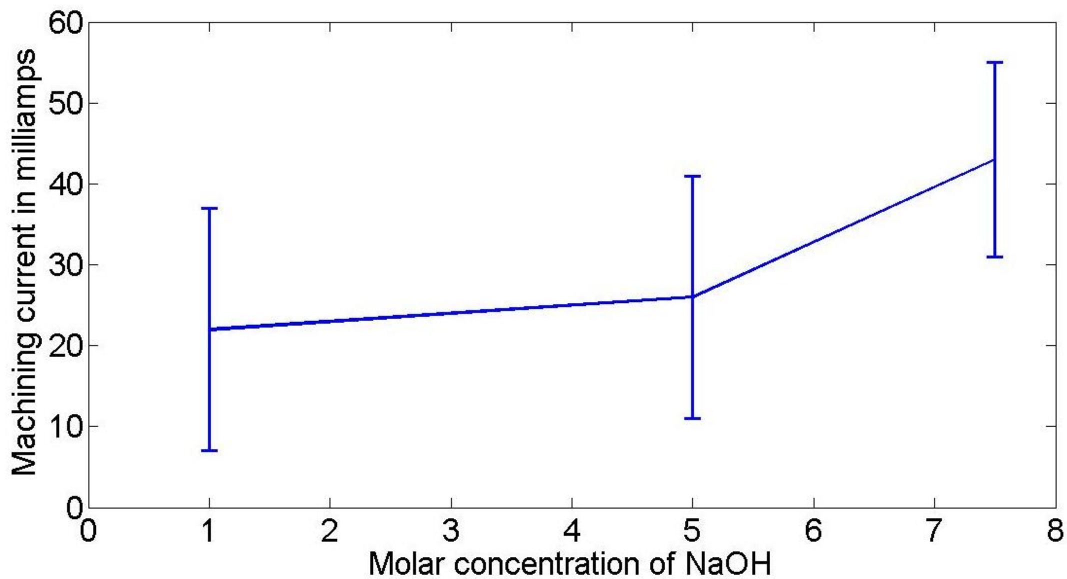

Figure 17: Machining current vs Electrolyte Concentration.

In order to measure the actual effect of electrolyte concentrations on overcut experiments were carried out using 1M, 5M and 7.5M NaOH. Borosilicate glass was used as the work material. The tool was kept in contact with the work piece during the experiments. No feed was provided during the experiments. The tool was not rotated during the experiments. Measurements were taken with machining times of 10 seconds, 60 seconds and 120 seconds at each concentration respectively. Each instance was repeated thrice to minimize the experimental errors. Table 3 explains the machining parameters used in the experiments.

Table 3: Machining parameters used to measure crater radius

Machining Parameter	Value
Machining Voltage	45V
Electrolyte	NaOH
Tool Material	Tungsten
Tool Diameter	300 µm
Immersion Depth	200 µm
Anode Material	Tool steel
Anode Dimensions	20 mm×20 mm×8 mm
Work Material	Borosilicate glass of 1mm thickness

4.4. Model verification

Aqueous sodium hydroxide reacts with glass at temperatures of 503°K. The reaction is rapid enough to do micromachining [43]. The room temperature is taken to be 303°K. So a temperature rise of 200°K is required for machining glass using sodium hydroxide.

The temperature distribution according to the radial distance (r) from the heat source (overcut) at varying times for 1M electrolyte concentration according to the model are shown in the figure 18 below. The value for the radial distance is the x-coordinate of the point on the curve corresponding to the machining temperature of 200°K.

The model explains the variation of overcut with respect to machining time. As expected overcut increases with machining time. Further the variation of temperature distribution with electrolyte concentration has also been captured. The machining results shown in figures 20 and 21 confirm that overcut increases with electrolyte concentration.

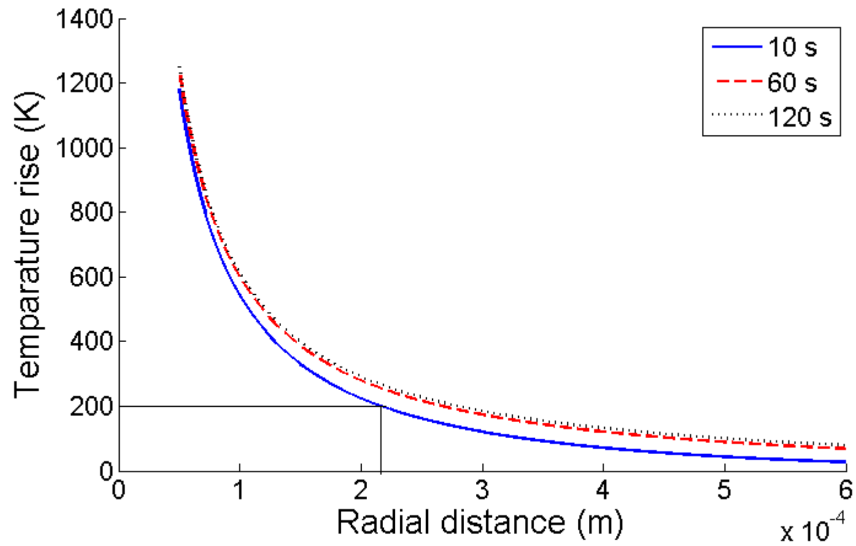

Figure 18: Variation in temperature rise along work piece with time.

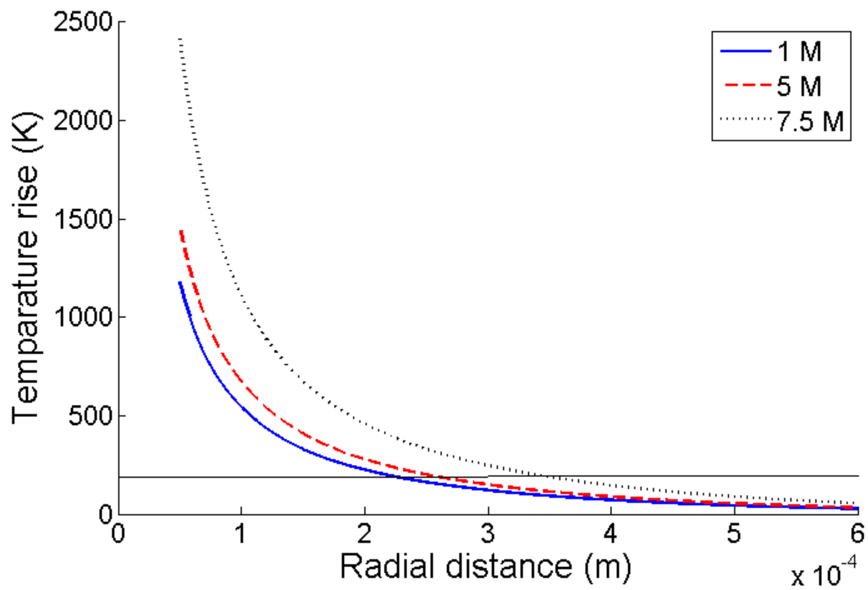

Figure 19: Variation in temperature rise along work piece with concentration.

The model was successfully able to predict overcut with maximum variation of 22%. The final experimental overcut was taken as the difference of the experimental value and the tool radius. The theoretical and experimentally predicted values for a constant tool diameter of 50 µm varied between 4-22%. The variation in experimental and predicted values is displayed in the figure 20.

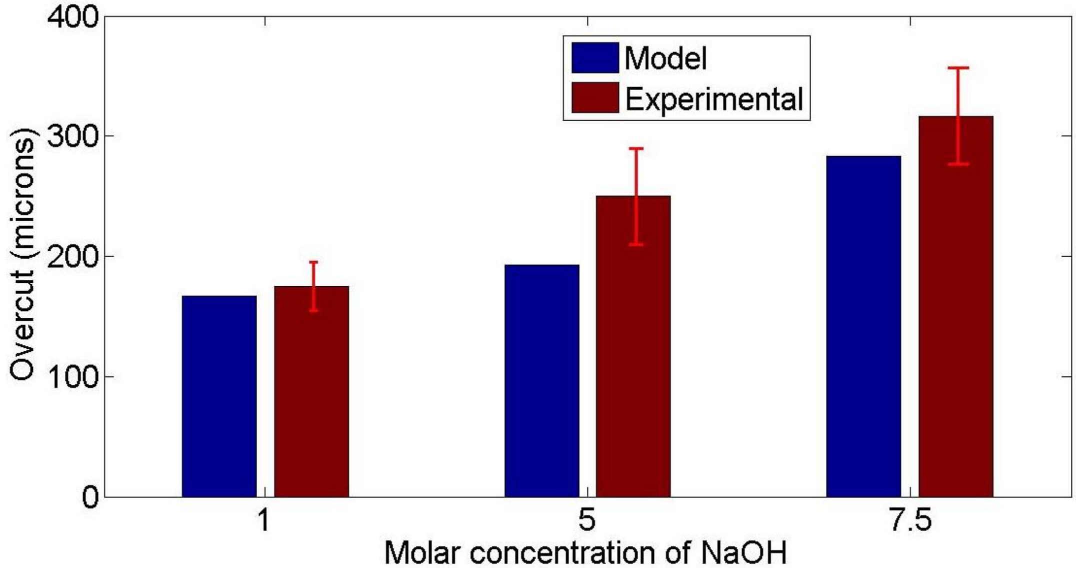

Figure 20: Comparison of model with experimental values using 50μm tools.

Experiments were also performed increasing the tool diameter to 300 μm. The theoretical and experimentally predicted values varied between 4–19%.

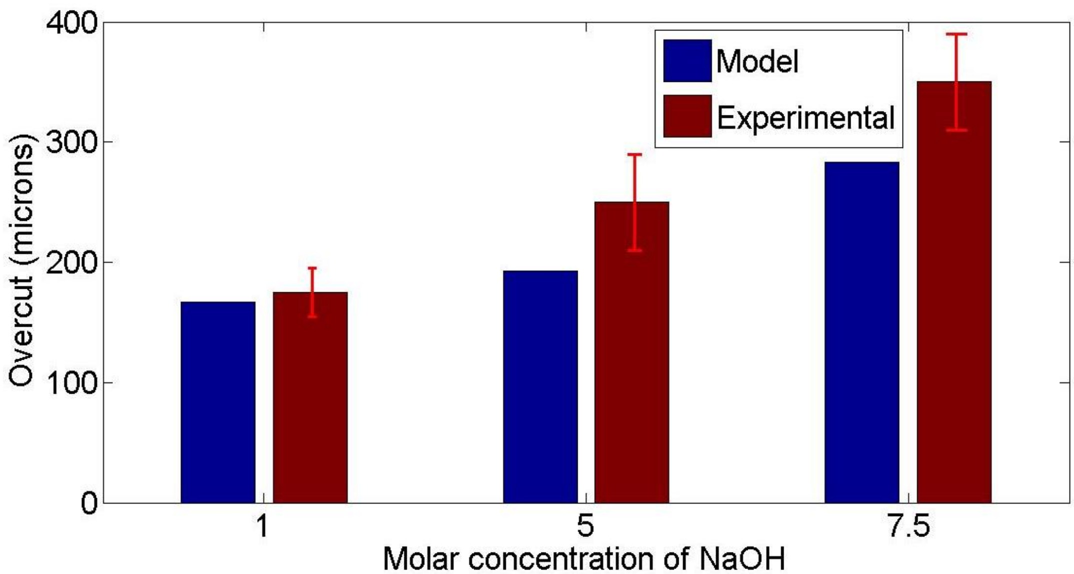

Figure 21: Comparison of model with experimental values using 300μm tools.

The experimental results confirm with the theoretical predictions that increase in electrolyte concentration increases overcut. We use this understanding in order to fabricate high aspect ratio microholes discussed in the next chapter.

CHAPTER 5

5. Fabrication of high aspect ratio microholes in glass using low electrolyte concentration

5.1. Introduction

The major issues with the deep hole drilling of micro holes in ECDM are:

- Lack of electrolyte circulation in the machining zone
- Damage to the machined surface due to high temperatures as a result of lack of heat dissipation resulting from non-availability of the electrolyte
- Tapered holes due to prolonged machining time resulting in large difference between entrance and exit diameters
- Fabrication of high aspect ratio microtools, and excessive tool wear in the micro sized tools

In this chapter, the feasibility of machining high aspect ratio micro holes in glass using micro ECDM has been investigated.

An overview of the aspect ratios of the holes machined on glass using ECDM by various research groups reported in the literature is listed in Table 4. In this table, aspect ratio is calculated as the ratio of depth to entrance diameter. As Yasuhiro et. al have made through holes, in this particular case, the aspect ratio is taken to be the ratio of depth to the average of the entrance and exit diameters.

Table 4: Aspect ratio of holes machined on glass by ECDM.

Reference	Diameter (μm)	Depth (μm)	Aspect Ratio
Cao et. al., 2009 [46]	60	150	2.5
Yasuhiro et. al., 2012 [16]	92	160	1.73
Han et. al., 2009 [47]	328	550	1.67
Zheng et. al., 2007 [25]	330	450	1.36
Cheng et. al., 2010 [48]	358	450	1.25
West et. al., 2007 [49]	430	500	1.16

It can be seen that the ability of ECDM to machine deep micro holes needs to be explored in order to expand the applications of glass. Following section describes the microtool fabrication and micromachining of high aspect ratio holes by ECDM using an in-house built experimental setup. The experimental results are discussed subsequently and finally conclusions are made from this study.

5.2. Fabrication of micro-tools

To machine high aspect ratio micro holes, high aspect ratio microtools are needed. The small tool sizes require a precise and reproducible microtool fabrication technique. Wire electro discharge grinding (WEDG) and micro electrodischarge machining (EDM) are the most widely used techniques to manufacture microtools. However, these processes suffer from defects due to surface deformation caused by residual stresses [50-53]. Microtool handling issues are minimized with the in-house production of micro tools in which the same experimental setup is used for the tool fabrication as well as the work piece machining using ECDM. Tungsten is a common tool material used in nontraditional micromachining processes such as electrodischarge machining, electrochemical machining, and ECDM. However, tungsten suffers from excessive tool wear especially in micromachining with extremely small tool sizes in the range of Ø 20-30 µm as shown in Figure 22.

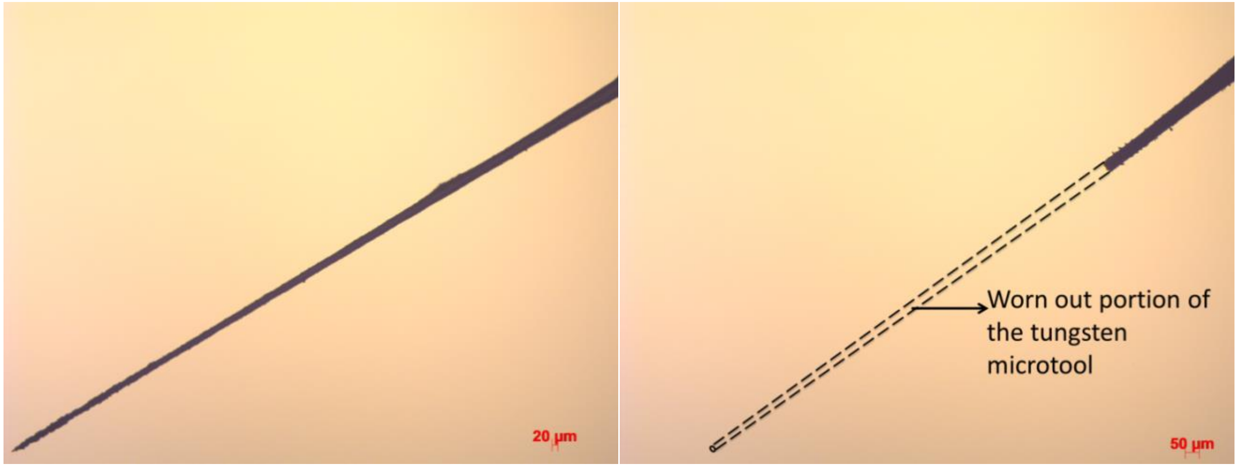

Figure 22: Microtool before and after machining.

In this study, tungsten carbide, which has better strength and corrosion resistance, is used as the tool material. The tungsten carbide microtool, shown in Figure 23, is fabricated by a pulse electrochemical micromachining (PECMM) process using the setup shown schematically in Figure 24.

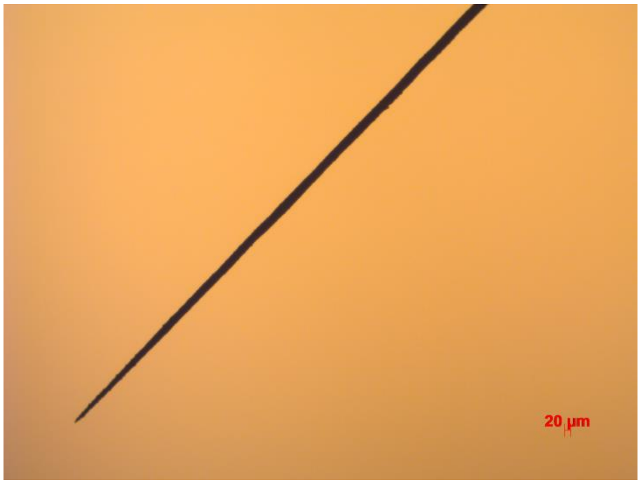

Figure 23: Tungsten Carbide microtool of Ø 30µm.

The tungsten carbide rods with diameters ranging from 20 to 30 µm were micromachined electrochemically for the subsequent ECDM studies.

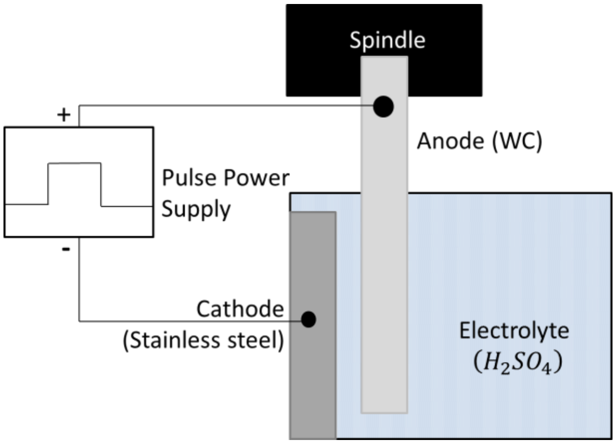

Figure 24: Schematic of microtool fabrication using PECMM.

The PECMM experimental parameters used for the tool fabrication are given in Table 5. Sulfuric acid was used as the electrolyte for the PECMM process as it was capable of effectively removing both tungsten and the cobalt binder present in the microtool [54]. Bipolar current was used during the microtool fabrication process, which eliminated the issue of tungsten passivation at acidic pH values [55, 56].

Table 5: PECMM parameters for tool fabrication.

Process Parameter	Value
Voltage	Forward – 4 V Reverse – 3 V
Anode	Tungsten carbide rod Ø300 μm
Cathode	0.5 mm thick stainless steel
Electrolyte	1M Sulfuric acid
Pulse On-Time	5 ms
Reverse pulse time	5 ms
Forward duty cycle	33%
Tool rotation	200 rpm

5.3. Experimental setup

The micro ECDM experimental setup used in this study is shown in figure 25. A rectangular tool steel block of dimensions 20 mm×20 mm×8 mm was used as the anode. The anode was kept at a distance of 5 cm from the cathode. The in-house fabricated tungsten carbide microtools were used as the cathode. The tools were cleaned using deionized water and then agitated in an ultrasonic bath of acetone for 2 minutes to remove the debris.

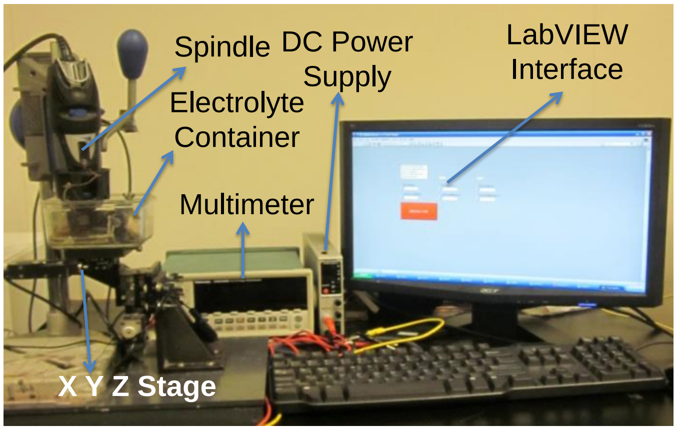

Figure 25: Experimental Setup.

The tool immersion depth was kept within the range of 300 µm as critical voltage increases with the same. A spindle capable of rotating at speeds upto 10,000 rpm was used in this study to rotate the microtool. A sensitive multimeter with a resolution of 0.01 milliamperes was used to monitor the current behavior during the machining process. This resolution was important as with the tool diameter in the range of 20-30 µm and the use of 1M NaOH the critical current varied in the range of a few milliamperes. A glass electrolyte container along with a fixture mechanism to hold the work piece was built in-house. A precision micro stage with a minimum step size of 0.1µm/s was used to provide the feed. The stage had a LabVIEW interface to control its position and movement. An optical measuring microscope and a scanning electron microscope were used to characterize the machined features. The current voltage characteristics were recorded to study their behavior using a 300 µm tungsten carbide tool in 1M NaOH. Figure 26 shows the variation of the current values with respect to voltage.

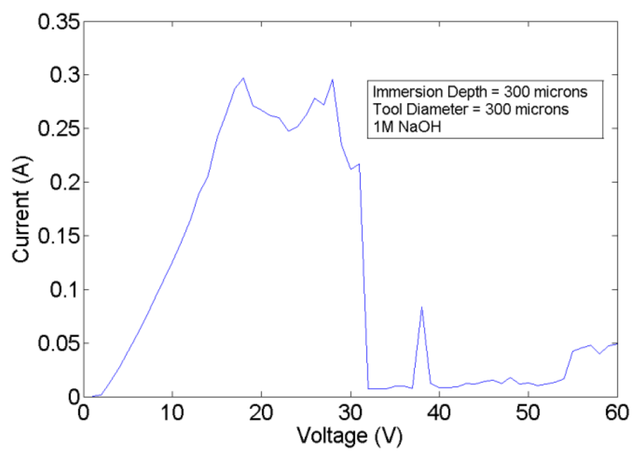

Figure 26: Experimental current Vs voltage characteristics.

5.4. Effect of tool rotation

To study the effect of tool rotation, micro holes were machined on a 200 µm sheet of glass at 45V using experimental parameters listed in Table 6. It was noticed that the circularity of the micro holes machined were better with tool rotation as shown in Figure 27. Figure 28 shows the effects of rotating the tool, on the critical voltage and current under varying electrolyte concentrations. The experiments were performed with a 300 µm tungsten tool and the immersion depth was kept constant at 500 µm.

Table 6: Experimental parameters for machining with and without tool rotation.

Process Parameter	Value
Anode	8 mm thick tool steel block
Cathode	Tungsten carbide rod Ø100 – Ø300 µm
Electrolyte	0.1 M, 2.5 M, 7.5 M NaOH
Tool rotation	0, 210, 1200, 2000, 2500 rpm
Work piece	200 µm thick glass slide

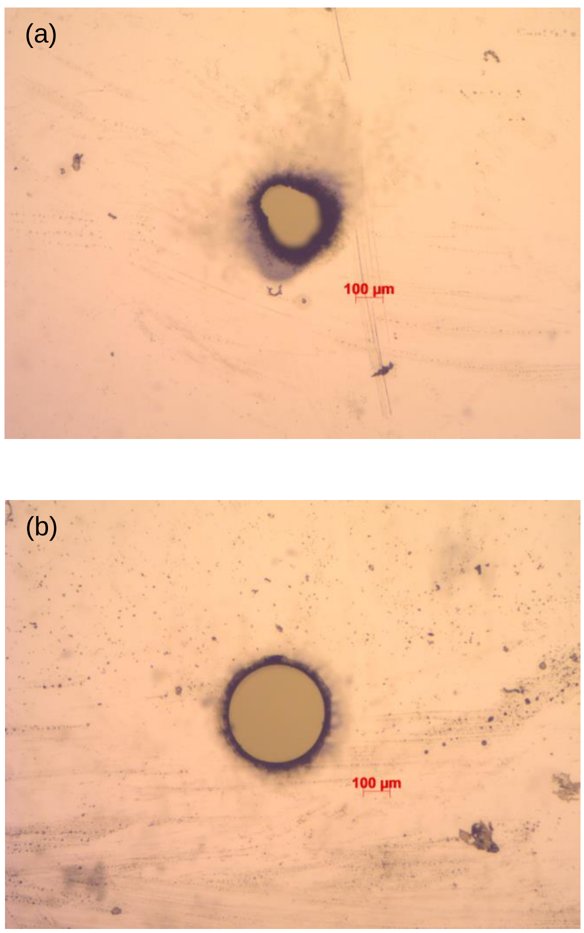

Figure 27: Tool rotation effects a) No Rotation b) With tool rotation at 1500 rpm.

The results show that tool rotation aids in the improvement of the hole circularity, but does not have significant effect on the critical voltage and critical current.

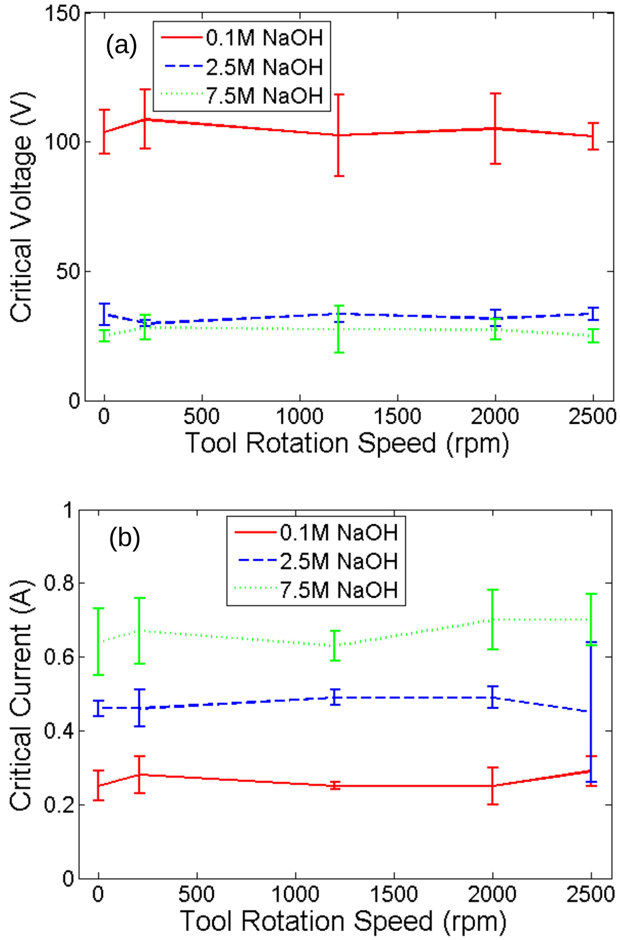

Figure 28: Effect of tool rotation on a) Critical Voltage and b) Critical current.

Experiments were performed with a 30 µm tungsten carbide tool using 1M, 1.5M and 2M concentrations of NaOH. In order to study the effect of concentration of the electrolyte on the hole diameters and the taper a constant voltage of 40V and feed rate of 1 µm/s was used to machine through holes on a glass plate of 1.2 mm thickness using these varying concentrations.

5.5. Effect of electrolyte concentration on entrance and exit diameters of the microholes

As the electrolyte concentration increased, the entrance and exit diameters of the microholes machined increased as well. Figure 29 shows the variation of the entrance and exit diameters with the electrolyte concentration. This effect can be explained by studying the material removal mechanism in ECDM. The heat supplied (P) by the discharges follow the equation,

$$P = (V - V_d) \times I - I^2 \times R$$

where,

V = machining voltage,

V_d= water decomposition potential,

I = mean current,

R = inter-electrode resistance

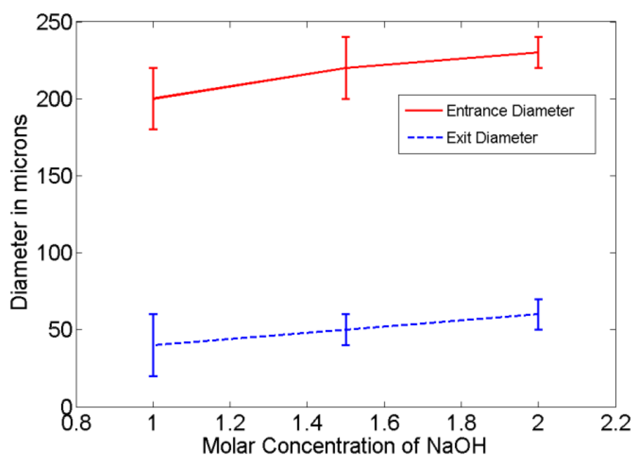

Figure 29: Effect of electrolyte concentration on the hole entrance and exit diameters.

The inter-electrode resistance is given by the ratio of mean voltage to mean current in the ohmic region. As the concentration of the electrolyte increases the inter-electrode resistance decreases. Hence, more energy is available for the machining process. Chemical reactions also contribute to this effect. The quality of the machined surface varies with the electrolyte used. Chemical etching of the work material is responsible for these observations. Silicon dioxide reacts with aqueous sodium hydroxide solution at elevated temperatures leading to etching of glass:

$$2NaOH + SiO_2 \rightarrow Na_2SiO_3 + H_2O$$

The etch rate increases with the strength of OH ions. These ions increase with the increase in the concentration of NaOH in the electrolyte. Thus, the increase in power as well as the availability of more OH ions leads to increase in the entrance and exit diameters.

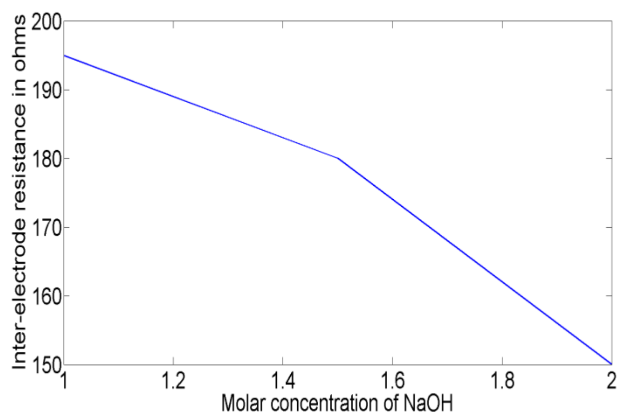

Figure 30: Variation of inter-electrode resistance with concentration.

5.6. Effect of concentration on overcut

The overcut was calculated as the difference between the average of the entrance and exit radii of the hole, and the tool radius which is 15 µm in this case. Figure 31 shows that the overcut increased with increase in concentration of the electrolyte. As explained before, due to the increase in entrance and exit diameters with concentration the overcut increases. Overcut plays a very important role in generating high aspect ratio features. The use of lower concentrations thus aids in increasing the aspect ratio of the machined features.

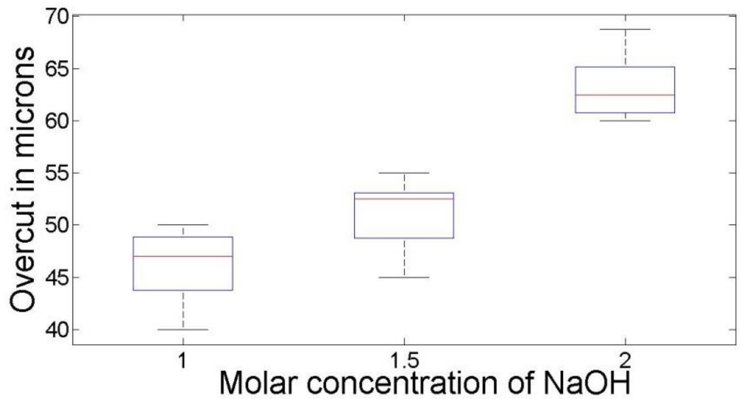

Figure 31: Effect of electrolyte concentration on overcut.

5.7. Effect of electrolyte concentration on micro hole taper

Micro hole taper is calculated as the ratio of difference between the entrance and the exit radii to the thickness of the glass plate. Figure 32 shows the increase in hole taper with the increase in the electrolyte concentration. As the top surface of the work material is exposed to the discharges for a longer period of time, more material is removed compared to the bottom layer. The increase in the number of OH ions due to increase in concentration result in a higher etch rate increasing the difference between the entrance and exit diameters.

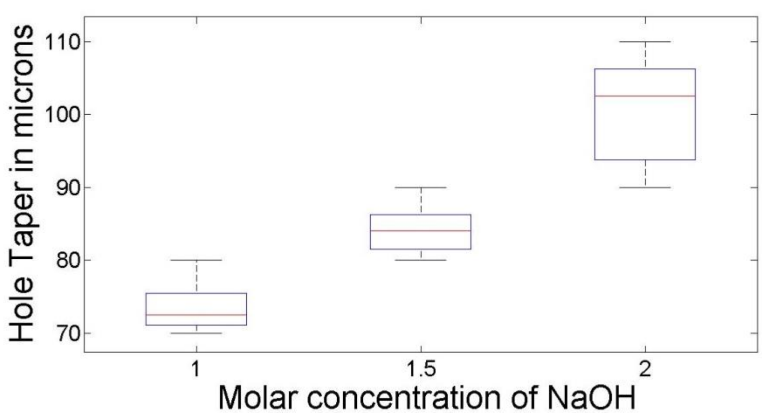

Figure 32: Effect of electrolyte concentration on hole taper.

5.8. Effect of electrolyte concentration on tool wear

Excessive tool wear drastically reduces tool length. As the length of the tool is important in machining deep micro holes, experiments were conducted to see the effect of concentration on the tool wear. Tungsten carbide tool of 30 µm was used for the study and the output voltage was kept at 40V. The machining time was kept constant at 30 minutes. Figure 33 shows the results of this study. The results show that tool wear reduces with the lowering of the electrolyte concentration. The heat transmitted to the work material increases with the concentration of the electrolyte. This heat is also responsible for eroding the tool.

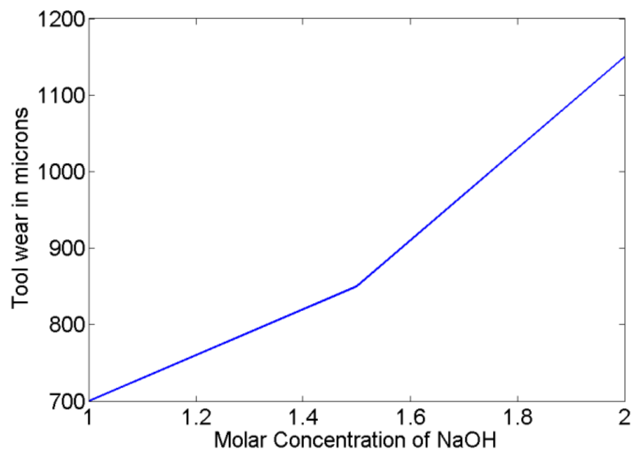

Figure 33: Effect of electrolyte concentration on tool wear.

5.9. Fabrication of high aspect ratio micro hole

Aspect ratio in this study is calculated as the ratio of the hole depth to the average of the entrance and exit diameters of the micro holes. By using a low concentration of electrolyte, the tool wear and overcut were reduced, enabling the high aspect ratio machining. Using 40 V DC power, 1 µm/s tool feed rate, and 1M NaOH a micro hole of entrance 180 µm and exit 40 µm was machined on a 1.2 mm borosilicate glass plate. Figure 34 shows the entrance and the exit diameters of the machined hole. This hole thus had an aspect ratio of 11 [57].

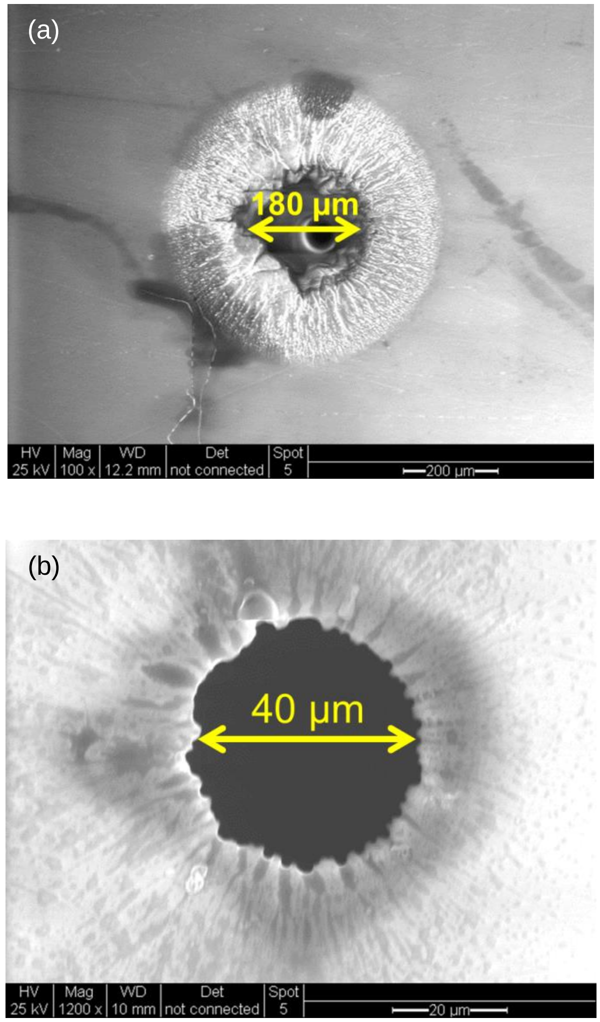

Figure 34: High aspect ratio microhole on 1.2 mm thick glass plate a) Entrance Ø180 µm b) Exit Ø40 µm.

5.10. Tolerance control and surface finish

Reducing tool wear and overcut enables better control over the tolerances of the machined features. The surface roughness of the machined samples was measured using an atomic force microscope. The surface roughness values varied from 250-350 nm and do not exhibit any particular trend. Therefore, no conclusion on the effect of concentration of electrolyte on surface roughness could be made with these results.

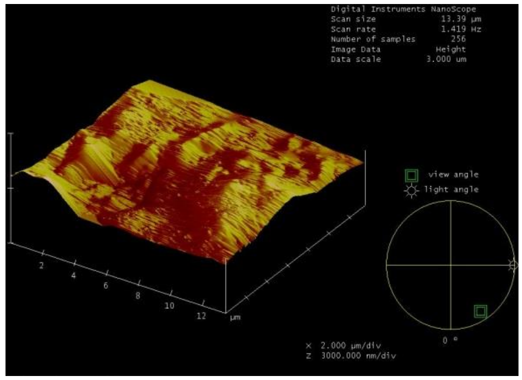

Figure 35: Atomic force microscope image of the machined surface with roughness value (Ra) of 250 nm.

CHAPTER 6

6. Conclusion and Future Work

6.1. Conclusion

A micro-ECDM setup was built as a part of this work. The system is capable of providing a feed rate of 1 μm/s. The current and voltage parameters could be recorded with the help of a LabVIEW interface. The preliminary micromachining studies involved microholes being fabricated on glass, silicon and barium titanate.

A mathematical model has been developed to quantify the effect of electrolyte concentration on the material removal mechanism. Experiments were carried out and the model was verified. The model shows that reducing the electrolyte concentration reduces machining overcut. It also shows that tool diameter has little effect on overcut at the micron scale. The model predicts overcut with a variation less than 22%.

Tungsten carbide microelectrodes fabricated using PECMM were used as microtools for the high aspect ratio micro ECDM of glass. It was found that rotation of the tool electrode improves the circularity of the machined hole, while not affecting the ECDM parameters like the critical voltage and the critical current. The study verified that using a lower concentration electrolyte of 1M reduces the overcut of the machined holes improving its aspect ratio as opposed to the concentrations of 2.5M, 5M and 7.5M reported in the literature. The overcut was reduced by 22% with the use of 1 M NaOH as the electrolyte. Hole taper was reduced by 18% and the tool wear by 39% due to the use of lower concentration of the electrolyte. An aspect ratio of 11 was achieved on glass with 1M NaOH and a 30 μm tungsten carbide tool fed at 1 μm/s using 40V. The surface roughness was found to be in the range of 250-350 nm.

Conclusions made from this work are:

- Performance of micro-ECDM is significantly affected by the concentration of the electrolyte

- Lowering the electrolyte concentration enables high aspect ratio micromachining. Aspect ratios in the range of 9 to 11 have been achieved.

6.2. Future Work

A control mechanism that senses contact between the tool and work material should be an immediate objective to take this research ahead. A suitable feedback signal should be decided upon and the controller should have a high response rate in order to react quickly. Such a mechanism would go a long way in maintaining the gap between the tool and work material machining deeper holes. As the gap is maintained electrolyte would be available in the machining zone providing good heat dissipation and resulting in excellent surface finish.

The chemical aspect of the material removal in ECDM has not been studied in detail yet. At higher depths the material removal mechanism is reported to be more of a chemical one. In order to quantify the material actually removed due to chemical action a mathematical model needs to be built. It would also advance the knowledge of the material removal mechanism in ECDM which is still not widely accepted.

High speed micromachining as well as the use of hollow tool electrodes with electrolyte flowing through could be used in order to increase the flow of electrolyte in the machining zone. Numerous feasibility studies could be conducted varying the machining parameters.

APPENDIX A: PUBLICATIONS / PRESENTATIONS

1) Jui, S.K., Kamaraj, A.B., and Sundaram, M.M., Fabrication of High Aspect Ratio Micro Holes in Glass by Micro Electrochemical Discharge Machining, NAMRI/SME, Vol. 41, 2013
2) Jui, S.K., Kamaraj, A.B., and Sundaram, M.M., High aspect ratio micromachining of glass by electrochemical discharge machining (ECDM), Journal of Manufacturing Processes, Special Edition, 2013
3) Jui, S.K., Kamaraj, A.B., Zicheng Cai and Sundaram, M.M., Study of high aspect ratio micromachining by electrochemical discharges, 2013 (In preparation)

REFERENCES

1. Aronson, R., *Micromanufacturing: The new frontier*. Manufacturing Engineering, 2007. 138(5): p. 89-100.
2. Mohd Abbas, N., D.G. Solomon, and M. Fuad Bahari, *A review on current research trends in electrical discharge machining (EDM).* International Journal of Machine Tools and Manufacture, 2007. 47(7–8): p. 1214-1228.
3. Bhattacharyya, B., S. Mitra, and A.K. Boro, *Electrochemical machining: new possibilities for micromachining.* Robotics and Computer-Integrated Manufacturing, 2002. 18(3–4): p. 283-289.
4. Clawson, A.R., *Guide to references on III–V semiconductor chemical etching.* Materials Science and Engineering: R: Reports, 2001. 31(1–6): p. 1-438.
5. Dubey, A.K. and V. Yadava, *Laser beam machining—A review*. International Journal of Machine Tools and Manufacture, 2008. 48(6): p. 609-628.
6. Singh, R. and J.S. Khamba, *Ultrasonic machining of titanium and its alloys: A review*. Journal of Materials Processing Technology, 2006. 173(2): p. 125-135.
7. Wüthrich, R. and V. Fascio, *Machining of non-conducting materials using electrochemical discharge phenomenon—an overview*. International Journal of Machine Tools and Manufacture, 2005. 45(9): p. 1095-1108.
8. Zhi-Ping Zheng, W.-H.C., Fuang-Yuan Huang,Biing-Hwa Yan, *3D microstructuring of Pyrex glass using the electrochemical discharge machining process.* Journal of Micromechanics and Microengineering, 2007. 17(5): p. 960.
9. Kim, D.-J., Ahn, Yoomin,Lee, Seoung-Hwan,Kim, Yong-Kweon, *Voltage pulse frequency and duty ratio effects in an electrochemical discharge microdrilling process of Pyrex glass.* International Journal of Machine Tools and Manufacture, 2006. 46(10): p. 1064-1067.
10. Abou Ziki, J. and R. Wüthrich, *Tool wear and tool thermal expansion during micro-machining by spark assisted chemical engraving.* The International Journal of Advanced Manufacturing Technology, 2012. 61(5-8): p. 481-486.

11. Cao, X.D., B.H. Kim, and C.N. Chu, *Micro-structuring of glass with features less than 100μm by electrochemical discharge machining.* Precision Engineering, 2009. 33(4): p. 459-465.

12. N.H. Cook, G.B.F., P. Jordan, B.N. Kalyani, *Experimental studies in electro-machining.* Transactions of ASME, Journal of Engineering for Industry, 1973: p. 945–950.

13. V.K. Jain, P.S.R., S.K. Choudhury, K.P. Rajurkar, *Experimental investigations into travelling wire electrocheimical spark machining (TW-ECSM) of composites.* Journal of Engineering for Industry, 1991(113): p. 75–84.

14. Wüthrich, R., *Chapter 8 - Designing a SACE Micromachining Set-up*, in *Micromachining Using Electrochemical Discharge Phenomenon*. 2009, William Andrew Publishing: Boston. p. 157-163.

15. H. Kurafuji, K.S., *Electrical discharge drilling of glass.* Annals of the CIRP, 1968(16): p. 415–419.

16. Mochimaru, Y.O., Minoru; Yamaguchi, Keishi, *Micro Hole Processing Using Electro-Chemical Discharge Machining.* Journal of Advanced Mechanical Design, Systems, and Manufacturing, 2012. 6(6): p. 949-957.

17. Tandon, S.J., V. K.;Kumar, P.;Rajurkar, K. P., *Investigations into machining of composites.* Precision Engineering, 1990. 12(4): p. 227-238.

18. Cook, N.F., GB;Jordan, P.;Kalyani, BN, *Experimental studies in electro-machining.* Journal of Engineering for Industry, 1973. 95: p. 945.

19. H. Langen, J.-M.B., H. Bleuler, Ph. Renaud, T. Masuzawa, *Micro electrochemical discharge machining of glass.* International Journal of Electrical Machining, 1998. 3: p. 65–69.

20. Wuthrich, R.F., V.;Viquerat, D.;Langen, H. *In situ measurement and micromachining of glass*. in *Micromechatronics and Human Science, 1999. MHS '99. Proceedings of 1999 International Symposium on*. 1999.

21. Eunice, S.L.D., Howard;Enzhu, Liang;Scott, D. Collins;Rosemary, L. Smith, *Removable tubing interconnects for glass-based micro-fluidic systems made using ECDM.* Journal of Micromechanics and Microengineering, 2004. 14(4): p. 535.

22. Gautam, N. and V.K. Jain, *Experimental investigations into ECSD process using various tool kinematics.* International Journal of Machine Tools and Manufacture, 1998. 38(1–2): p. 15-27.

23. C.T. Yang, S.S.H., B.H. Yan, *Micro hole machining of borosilicate glass trough electrochemical discharge machining (ECDM).* Key Engineering Materials, 2001(196): p. 149–166.

24. Jain, V.K., S.K. Choudhury, and K.M. Ramesh, *On the machining of alumina and glass.* International Journal of Machine Tools and Manufacture, 2002. 42(11): p. 1269-1276.

25. Zhi-Ping, Z., Hsin-Chuan, Su Fuang-Yuan, Huang Biing-Hwa, Yan, *The tool geometrical shape and pulse-off time of pulse voltage effects in a Pyrex glass electrochemical discharge microdrilling process.* Journal of Micromechanics and Microengineering, 2007. 17(2): p. 265.

26. Yang, C.-K.W., Kun-Ling Hung, Jung-Chou Lee, Shin-Min Lin, Jui-Che Yan, Biing-Hwa, *Enhancement of ECDM efficiency and accuracy by spherical tool electrode.* International Journal of Machine Tools and Manufacture, 2011. 51(6): p. 528-535.

27. M. Mousa, A.A., H. D. Ng, R. Wüthrich, *The effect of thermal conductivity of the tool electrode in spark-assisted chemical engraving gravity-feed micro-drilling.* Journal of Micromechanics and Microengineering, 2009. 19(1): p. 015010.

28. Min-Seop, H., B.-K. Min, and S.-J. Lee. *Reduction of Overcut in the Electrochemical Discharge Machining Process Using a Side-insulated Electrode*. in *Smart Manufacturing Application, 2008. ICSMA 2008. International Conference on*. 2008.

29. Han, M.-S., B.-K. Min, and S.J. Lee, *Modeling gas film formation in electrochemical discharge machining processes using a side-insulated electrode.* Journal of Micromechanics and Microengineering, 2008. 18(4): p. 045019.

30. Basak, I. and A. Ghosh, *Mechanism of spark generation during electrochemical discharge machining: a theoretical model and experimental verification.* Journal of Materials Processing Technology, 1996. 62(1–3): p. 46-53.

31. Basak, I. and A. Ghosh, *Mechanism of material removal in electrochemical discharge machining: a theoretical model and experimental verification.* Journal of Materials Processing Technology, 1997. 71(3): p. 350-359.

32. Liu, J.W., T.M. Yue, and Z.N. Guo, *An analysis of the discharge mechanism in electrochemical discharge machining of particulate reinforced metal matrix composites.* International Journal of Machine Tools and Manufacture, 2010. 50(1): p. 86-96.

33. Fascio, V., R. Wüthrich, and H. Bleuler, *Spark assisted chemical engraving in the light of electrochemistry*. Electrochimica Acta, 2004. 49(22–23): p. 3997-4003.

34. Wüthrich, R. and H. Bleuler, *A model for electrode effects using percolation theory.* Electrochimica Acta, 2004. 49(9): p. 1547-1554.

35. Wüthrich, R., V. Fascio, and H. Bleuler, *A stochastic model for electrode effects.* Electrochimica Acta, 2004. 49(22): p. 4005-4010.

36. Wüthrich, R.H., LA Lal, Ashwin Fujisaki, K Bleuler, Hannes Mandin, Ph Picard, Gérard, *Physical principles and miniaturization of spark assisted chemical engraving (SACE).* Journal of Micromechanics and Microengineering, 2005. 15(10): p. S268.

37. Wüthrich, R. and L. Hof, *The gas film in spark assisted chemical engraving (SACE)—a key element for micro-machining applications.* International Journal of Machine Tools and Manufacture, 2006. 46(7): p. 828-835.

38. Vogt, H., *The anode effect as a fluid dynamic problem.* Journal of Applied Electrochemistry, 1999. 29(2): p. 137-145.

39. Bhondwe, K., V. Yadava, and G. Kathiresan, *Finite element prediction of material removal rate due to electro-chemical spark machining.* International Journal of Machine Tools and Manufacture, 2006. 46(14): p. 1699-1706.

40. Wei, C.X., Kaizhou Ni, Jun Brzezinski, Adam John Hu, Dejin, *A finite element based model for electrochemical discharge machining in discharge regime.* The International Journal of Advanced Manufacturing Technology, 2011. 54(9): p. 987-995.

41. Jain, V.K. and S. Adhikary, *On the mechanism of material removal in electrochemical spark machining of quartz under different polarity conditions.* Journal of Materials Processing Technology, 2008. 200(1–3): p. 460-470.

42. Wüthrich, R., *Chapter 5 - Material Removal Mechanism*, in *Micromachining Using Electrochemical Discharge Phenomenon*. 2009, William Andrew Publishing: Boston. p. 97-113.

43. Jendoubi, F., A. Mgaidi, and M. El Maaoui, *Kinetics of the dissolution of silica in aqueous sodium hydroxide solutions at high pressure and temperature.* The Canadian Journal of Chemical Engineering, 1997. 75(4): p. 721-727.

44. Janssen, L. and M. Warmoeskerken, *Transport phenomena data companion*. 1987: E. Arnold.

45. H.S. Carslaw, J.C.J., *Conduction of heat in solids.* 1947: p. 386.

46. Cao, X.D., Kim, Bo Hyun, Chu, Chong Nam, *Micro-structuring of glass with features less than 100μm by electrochemical discharge machining.* Precision Engineering, 2009. 33(4): p. 459-465.

47. Min-Seop, H., M. Byung-Kwon, and L. Sang Jo, *Geometric improvement of electrochemical discharge micro-drilling using an ultrasonic-vibrated electrolyte.* Journal of Micromechanics and Microengineering, 2009. 19(6): p. 065004.

48. Cheng, C.-P.W., Kun-Ling Mai, Chao-Chuang Hsu, Yu-Shan Yan, Biing-Hwa, *Magnetic field-assisted electrochemical discharge machining.* Journal of Micromechanics and Microengineering, 2010. 20(7): p. 075019.

49. Jonathan, W. and J. Amol, *ECDM methods for fluidic interfacing through thin glass substrates and the formation of spherical microcavities.* Journal of Micromechanics and Microengineering, 2007. 17(2): p. 403.

50. Tae-Hyun, J., P. Kyu-Yeol, and L. Won-Kyu. *A study on the micro electric discharge grinding characteristics of WC-Co-relationship between surface integrity and dielectric conditions*. in *Science and Technology, 2000. KORUS 2000. Proceedings. The 4th Korea-Russia International Symposium on*. 2000.

51. Liu, H.S.Y., Biing Hwa Chen, Chien Liang Huang, Fuang Yuan, *Application of micro-EDM combined with high-frequency dither grinding to micro-hole machining.* International Journal of Machine Tools and Manufacture, 2006. 46(1): p. 80-87.

52. Kunieda, M.L., B. Rajurkar, K. P. Schumacher, B. M., *Advancing EDM through Fundamental Insight into the Process.* CIRP Annals - Manufacturing Technology, 2005. 54(2): p. 64-87.

53. Liu Y., Z.F., Sundaram M.M., and Rajurkar K.P., *Study on the Surface Integrity of Machined Tool in Micro EDM.* Proceedings of the 16th international symposium on electromachining, 2010. (ISEM XVI): p. p. 685-689.

54. Choi, S.H.R., S. H. Choi, D. K. Chu, C. N., *Fabrication of WC micro-shaft by using electrochemical etching.* The International Journal of Advanced Manufacturing Technology, 2007. 31(7-8): p. 682-687.

55. Mathew, R. and M.M. Sundaram, *Modeling and fabrication of micro tools by pulsed electrochemical machining.* Journal of Materials Processing Technology, 2012. 212(7): p. 1567-1572.

56. Balsamy Kamaraj, A., R. Dyer, and M.M. Sundaram. *Pulse Electrochemical Micromachining of Tungsten Carbide*. in *ASME 2012 International Manufacturing Science and Engineering Conference (MSEC2012)* 2012. University of Notre Dame, Notre Dame, IN, USA.

57. Jui, S.K., Kamaraj, A.B., and Sundaram, M.M., *Fabrication of High Aspect Ratio Micro Holes in Glass by Micro Electrochemical Discharge Machining.* NAMRI/SME, 2013. Vol. 41.